Journal of Groundwater Science and Engineering 14(2026) 188–198

Journal homepage: http://gwse.iheg.org.cn

Research Article

Evaluation of the effect of ultrasonic waves on nitrate removal from aqueous solutions using Zinc- and Iron- coated activated carbon

Mohammad Reza Alashti[1], Mojtaba Khoshravesh[1*], Fardin Sadegh-Zadeh[2], Hazi Mohammad Azamathulla[3]

[1] *Department of Water Engineering, Faculty of Agronomy Engineering, Sari Agricultural Sciences and Natural Resources University, Sari, Iran.*
[2] *Department of Soil Science, Faculty of Agronomy, Sari Agricultural Sciences and Natural Resources University, Sari, Iran.*
[3] *Department of Civil and Environmental Engineering, University of the West Indies at St. Augustine, Trinidad, Trinidad and Tobago.*

Abstract: Nitrate contamination in water represents a significant threat to both public health and the environment. While ultrasonic technology has emerged as an eco-friendly approach with potential for enhancing nitrate removal, its full capacity remains underexplored. This study aims to assess the effectiveness of ultrasound in improving nitrate removal from aqueous solutions using biochar derived from rice straw, modified with Fe^{3+} and Zn^{2+} as cationic bridges. Conducted at the water quality laboratory of Sari Agricultural Sciences and Natural Resources University, the experiments revealed that iron-coated biochar treatments (BF and BFU) exhibited outstanding performance in nitrate removal. Ultrasound application significantly enhanced nitrate removal efficiency, with the combination of ultrasonic waves and iron-coated biochar (BFU) achieving a maximum adsorption capacity (q_m) of 3.664 mg/g, which surpassed non-sonicated treatments (BF: 3.345 mg/g) and reduced equilibrium time by 92% (from 60 min to 5 min). Furthermore, ultrasonic treatment improved the performance of Zn^{2+}-coated biochar (BZU), boosting removal rates by more than 25% through cavitation-induced particle fragmentation and enhanced mass transfer. Mechanistic analysis indicated that ultrasound facilitates the homogenization of the adsorption surface, favoring Langmuir-type monolayer adsorption ($R^2 > 0.95$), while the cationic bridges (Fe^{3+}/Zn^{2+}) strengthened electrostatic interactions with nitrate ions. Under optimized conditions, the combination of ultrasound and cation-modified biochar achieved over 90% nitrate removal, presenting a promising, energy-efficient, and sustainable solution for water treatment. These findings demonstrate the potential of ultrasonic-assisted, cation-modified biochar as a highly effective strategy for mitigating nitrate contamination in water systems.

Keywords: Biochar; Iron coating; Langmuir model; Water quality; Zinc coating

Received: 15 Jan 2025/ Accepted: 02 Dec 2025/ Published: 30 Apr 2026

Introduction

Discharge of water and wastewater with high nitrate concentrations into groundwater is a global concern. Recent studies have shown that such contamination contributes to the proliferation of harmful cyanobacteria, posing risks to drinking water safety and aquatic biodiversity. For example, Nguyen Le et al. (2024) showed that high levels of nitrogen can rapidly stimulate cyanobacterial blooms, leading to higher concentrations of cyanotoxins in freshwater systems. This issue has been exacerbated over the past century due to nutrient loads from intensive agricultural practices and municipal sewage discharges, causing eutrophication and hypoxia in aquatic ecosystems, and becoming a significant societal concern (Reusch et al. 2018). Lahjouj et al. (2020) evaluated nitrate contamination in the plioquaternary aquifer of the Sais Basin using a statistical approach. Samples from agricultural areas were collected during spring and autumn of 2018, revealing that 55% and

*Corresponding author: Mojtaba Khoshravesh, *E-mail address*: khoshravesh_m24@yahoo.com

DOI: 10.26599/JGSE.2026.9280078

Alashti MR, Khoshravesh M, Sadegh-Zadeh F, et al. 2026. Evaluation of the effect of ultrasonic waves on nitrate removal from aqueous solutions using Zinc- and Iron- coated activated carbon. Journal of Groundwater Science and Engineering, 14(2): 188-198.

57% of the samples, respectively, exceeded the WHO threshold (50 mg/L). Statistical analyses, including correlation matrix and principal component analysis, indicate that nitrate pollution is linked to anthropogenic sources. Although nitrate itself is not acutely toxic, its microbial reduction to nitrite in the gastrointestinal tract can cause methemoglobinemia, a condition that impairs the oxygen-carrying capacity of blood, particularly dangerous in infants. Furthermore, nitrite may react with dietary amines to form N-nitroso compounds, which are classified as probable human carcinogens. Due to these risks, the World Health Organization (WHO) has set a guideline value of 50 mg/L nitrate (as NO_3^-) in drinking water to protect public health (Ward et al. 2024). Therefore, removal of nitrate ions from water is necessary to mitigate these health risks.

Currently, various methods are utilized for the removal of nitrate ions from water, including ion exchange, coagulation-precipitation, membrane processes, electrochemical techniques, electrocoagulation, and biological treatments. However, adsorption—particularly using biochar—has received increasing attention due to its high efficiency, low cost, operational simplicity, and environmental compatibility. Recent studies have shown that metal-modified biochars, especially those doped with iron and nitrogen, significantly enhance nitrate adsorption performance. For instance, iron- and nitrogen-doped biochar produced at 800°C exhibited a maximum nitrate adsorption capacity of 20.67 mg/g, highlighting its strong potential for water purification applications (Mood et al. 2024).

Hosseingholilu et al. (2019) reported that ultrasound technology is among the latest advancements in the desalination industry, enhancing the evaporation and distillation processes by improving mass and heat transfer, ultimately reducing energy consumption. Moreover, this technology offers the advantage of chemical-free treatment, ensuring a healthy and safe approach.

Radicals and molecules such as H, OH, and H_2O_2, known as highly potent oxidizing agents, are formed through the breakdown of water molecules (pyrolysis) under extreme conditions. These cavitation bubbles continue to expand during compression and degradation cycles until they reach a critical size, leading to their eventual collapse in the subsequent compression phase. Zameni et al. (2016) conducted a study on nitrate removal from aqueous solutions using an iron (III)-coated rice straw biochar adsorbent. The results of their isotherm test indicated that the nitrate adsorption process followed the Langmuir isotherm linear model, and the maximum nitrate adsorption capacity was found to be 43.66 mg/g. Rashwan et al. (2020) studied the kinetics of hydrogen production using sonication energy in water and attributed the increase in hydrogen production to the rate of temperature increase in microbubbles obtained through ultrasonication. A recent study by Guo et al. (2023) investigated the effectiveness of ultrasonic vibration in removing ammonia nitrogen from aquaculture water. The researchers found that the use of ultrasonic waves significantly increased the efficiency of ammonia nitrogen removal, especially at low concentrations. This study demonstrated that ultrasonic treatment can effectively reduce ammonia levels, making it a promising method for water treatment in aquaculture systems. In a recent study by Janajreh et al. (2022), the effect of ultrasonic parameters on the performance of Direct Contact Membrane Distillation (DCMD) was investigated. The researchers developed an ultrasonic DCMD module equipped with a commercial PTFE membrane and conducted experiments to evaluate the effects of different ultrasonic frequencies and amplitudes on mass transfer. The findings showed that the use of ultrasound at an intensity of 4,525 W/m^2 increased the mass flux from 4.25 L/m^2·h to 8.1 L/m^2·h, corresponding to a 90% increase. This improvement was attributed to the disruption of the kinetic and thermal boundary layers due to ultrasonic-induced mixing. Mohamad Aris et al. (2018) explored and evaluated the effect of ultrasonic irradiation on nitrogen ammonia removal, considering parameters such as initial concentration, pH, and radiation time of waves.

Due to the negative electric charge on biochar, the adsorption of anionic materials such as nitrate is not highly effective. However, the use of cationic bridges to enhance the adsorption rate of anions in this type of adsorbent is of particular interest. Additionally, ultrasonic waves can produce hydrogen as one of their products, which may be effective in the reduction and adsorption of nitrate by biochar. Ultrasound has been shown to significantly increase the efficiency of nitrate removal by intensifying the cavitation phenomenon. During ultrasound, the formation and collapse of microscopic bubbles creates high temperatures and pressures, which in turn produce reactive species that facilitate the degradation of nitrate ions. Notably, the duration of ultrasonic exposure plays an important role, as longer exposure times lead to increased cavitation intensity and improved pollutant degradation (Dehghani et

al. 2023; Serena Galvez et al. 2022). Nevertheless, the simultaneous use of ultrasonic waves and biochar adsorbent (BU) coated with iron (III) (BFU) and zinc (BZU) as cationic bridges for reducing nitrate pollutants in agricultural effluents has not been explored in previous studies. Therefore, the main objective of this study was to examine how ultrasound technology influences the removal of nitrate from water using biochar made from rice straw and enhanced with Fe^{3+} and Zn^{2+} as cationic bridges. A key innovation in this study is the exploration of a synergistic interaction between iron/zinc-coated biochar and ultrasonic waves, a combination not previously studied for nitrate removal. This integrated approach utilizes both physical and chemical mechanisms to enhance nitrate adsorption.

1 Materials and methods

1.1 Biochar production

Inexpensive rice straw materials were utilized for the production of biochar. The chopped straw was placed inside an electric furnace and heated for one hour until reaching the desired temperature. Subsequently, it was maintained at that temperature for 2 hours. This research focused on producing biochar at two different temperatures, 350°C and 650°C. The resulting biochar was then washed three times with distilled water at a ratio of 1:20 and dried in an oven at 70°C for 24 hours.

1.2 Biochar coating

To coat the biochar, solutions were prepared by dissolving $ZnCl_2$ and $FeCl_3$ in distilled water. Concentrations of 1,000 ppm and 10,000 ppm were used for Fe^{3+}, while concentrations of 10,000 ppm, 30,000 ppm, and 40,000 ppm were used for Zn^{2+}. Once the solutions were ready, the biochar was mixed into the solutions at a ratio of one gram of adsorbent to 50 mL of solution. The mixture was then shaken on a shaker for 24 hours. Subsequently, the coated adsorbents were washed three times with distilled water at a ratio of 1:20 and dried in an oven at 70°C for 24 hours.

1.3 Ultrasonic device

In this study, the Ultrasonic Processing model FS-450 ultrasonic device with a frequency of 20 kHz and a power of 450 W was employed to generate ultrasound waves. During the experiments involving ultrasonication, the samples mixed with the adsorbent were exposed to ultrasonic waves for a duration of 5 minutes.

1.4 Methods of determining nitrate in solution

After filtering the samples using filter papers and syringe filters, two methods were employed to measure the remaining amount of nitrate in the test solutions. In the first method, the APHA (2012) Section 4500 $NO_3^- B$ method, the filtered samples were centrifuged for 5 minutes at 12,000 rpm. The second method used was the Cataldo et al. (1975) method. The SP-UV 300SRB model spectrophotometer was used to read the samples and determine the extent of nitrate adsorption from the solutions. Control samples without biochar were also included in the study.

1.5 Procedures for conducting experiments

These experiments were conducted at a temperature of 25 ± 1°C, and each experiment was replicated three times. Throughout the experiments, optimal conditions obtained from the previous stages were used. In the first stage, equilibrium time tests were conducted for three adsorbents: biochar, biochar coated with Fe (III), and biochar coated with Zn (II). The tests were performed at intervals of 10, 30, 60, 120, 180, 240, and 300 minutes. For each test, exactly 0.5 grams of the adsorbent and 40 cc of nitrate solution with a concentration of 80 ppm were placed in a centrifuge tube and stirred on a shaker for the specified period of time. In the second step, the adsorption of nitrate was examined at different pH levels. The tests were performed at the equilibrium times obtained in the first stage, and pH values of 2, 4, 6, 7, 8, and 10 were investigated to determine the optimal pH. Next, experiments were conducted to determine the optimal dosage of adsorbents. Different amounts of 0.2, 0.4, 0.6, 0.8, and 1 gram of adsorbents were used for this purpose. Subsequently, adsorption isotherms were determined using nitrate solutions with concentrations of 20, 45, 80, 100, 150, and 200 ppm, following the optimal conditions obtained earlier. In the experiments combined with ultrasonic treatment, equilibrium time tests were performed at 3 and 5 minutes. To evaluate and compare the adsorption capacities of biochar, biochar coated with Fe (III), and biochar coated with Zn (II) for nitrate, the Langmuir and

Freundlich isotherms were used to fit the sorption data. The equation for Langmuir's adsorption isotherm is as follows:

$$\text{Langmuir}, C_e/q_e = 1/bq_m + C_e/q_m \quad (1)$$

Where: C_e is the equilibrium concentration of nitrate in solution ($mg \cdot L^{-1}$); q_e is the amount of the nitrate adsorbed per unit weight of biochar ($mg \cdot g^{-1}$); b is the constant related to the affinity and q_m is the maximum adsorption capacity ($mg \cdot g^{-1}$). A straight line is obtained by plotting $1/q_e$ against $1/C_e$, where q_e is determined from the slope (b) and the intercept (q_m) with the y-axis of the graph.

The equation for Freundlich's model is as follows:

$$\log q_e = \log k_f + (1/n_f)\log C_e \quad (2)$$

Where: k_f $((mg/g)(L/mg)^{\frac{1}{n}})$ and n_f (dimensionless) are the constants that are related to adsorption capacity and adsorption intensity, respectively. The adsorption capacity, k_f, accurately describes the adsorption data in practical terms, enabling the investigation of the adsorbents' capacity for the pollutant. When examining the Freundlich model, plotting $\log q_e$ against $\log C_e$ yields a straight line, and the slope and intercept of this line correspond to $1/n_f$ and k_f, respectively.

2 Results and discussion

2.1 Results of preliminary experiments comparing biochars

The results indicated that biochars produced at a temperature of 350°C, as well as those coated with Fe^{3+} and Zn^{2+} at this temperature, exhibited poor performance in nitrate adsorption. Similarly, among the biochars produced at a temperature of 650°C, those coated with solutions containing 1,000 ppm of Fe^{3+} and 10,000 ppm or 30,000 ppm of Zn^{2+} also did not show satisfactory performance. Consequently, three effective adsorbents, namely biochar (B), biochar coated with 10,000 ppm Fe^{3+} solution (BF), and biochar coated with 40,000 ppm Zn^{2+} solution (BZ) (all produced at a temperature of 650°C), were selected for further experimentation.

2.2 The effect of ultrasonic times

The results of the preliminary tests indicated that ultrasonic applications for a duration of 5 minutes exhibited better performance compared to applications for 3 minutes. As a result, the duration of ultrasonic application in other related experiments was set to 5 minutes.

2.3 Effect of equilibrium time on nitrate adsorption

Experiments were conducted to determine the equilibrium time for three adsorbents: B, BZ, and BF. The equilibrium times chosen for B, BF, and BZ were 60, 60, and 120 minutes, respectively. The results of these experiments are illustrated in Fig. 1.

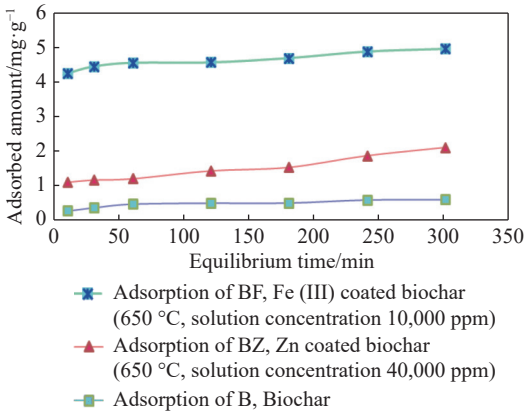

Fig. 1 The amounts of nitrate adsorbed by B, BZ, and BF from solutions at different time intervals

2.4 The effect of solution pH on nitrate adsorption

Aqueous pH not only influences the chemical speciation of ions but also alters the surface charge on biochar surfaces through protonation and deprotonation of surface functional groups, thereby impacting ion adsorption processes (Zhang et al. 2020). pH is a crucial parameter controlling all stages of adsorption, affecting the speciation of nitrate and the surface charge of the adsorbent during the adsorption process. The increase in adsorption is attributed to the enhanced electrostatic attraction between the adsorbent and the adsorbed ions (Zameni et al. 2016). The amounts of nitrate adsorbed at different pH levels are presented in Fig. 2.

The amount of adsorbed nitrate increased as the solution's pH decreased for the adsorbents, reaching the maximum adsorption at pH levels of 2 and 4. Recent studies have shown that the efficiency of nitrate adsorption is significantly affected by the pH of the solution and the presence of competing anions. At lower pH levels, the adsorbent surfaces

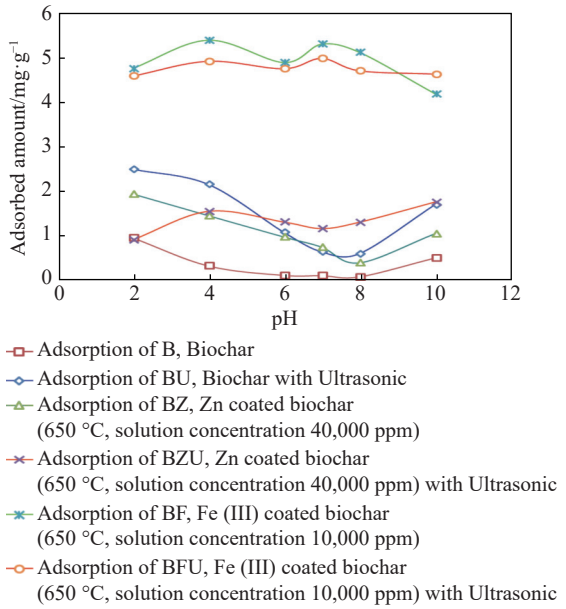

Fig. 2 The amounts of Nitrate adsorbed by the B, BU, BZ, BZU, BF and BFU from solutions at different pH

become positively charged, increasing the electrostatic attraction between the adsorbent and the negatively charged nitrate ion, thereby increasing the adsorption efficiency. Conversely, at higher pH values, the adsorbent surfaces acquire negative charges, leading to electrostatic repulsion with nitrate ions, thereby reducing the adsorption efficiency. In addition, hydroxide ions (OH^-) present at higher pH levels compete with nitrate ions for adsorption sites, further reducing the efficiency of nitrate removal. The presence of other anions such as phosphate (PO_4^{3-}) and sulfate (SO_4^{2-}) can also compete with nitrate ions for adsorption sites, thereby reducing the nitrate adsorption capacity, consistent with the findings of Zameni et al. (2016), Kumar and Singh (2024), and Sharma and Gupta (2024). The pH of the solution not only influenced the surface charge and dissociation of functional groups but also impacted the degree of ionization, determining the adsorption behavior of the adsorbent (Hu et al. 2015). The experimental results demonstrated that the performance of the adsorbents decreased with increasing pH.

At higher pH levels, OH^- ions may compete with nitrate for adsorption sites on the biochar surface. It has been demonstrated that protonation of biochar surface functional groups at low pH results in an increase in positive surface charge, which is believed to enhance nitrate sorption. The optimum pH values obtained in this research for nitrate adsorption are 4, 7, and 10 for BF, BFU, and BZU, respectively, while it is 2 for BU, B, and BZ.

2.5 Effect of adsorbent dosage on nitrate adsorption

The amount of nitrate adsorbed at different adsorbent doses is presented in Fig. 3. The optimal adsorbent dose obtained for BZU and BU is 0.3 grams, while for BFU, BF, BZ, and B, it is 1 gram.

The initial concentration of the solution is another important and influential factor in the process of nitrate adsorption by adsorbents. The higher maximum adsorption capacity in biochars with iron coating is attributed to the fact that most of the biochar surface carries a negative charge, while Fe (III) with its positive charge is adsorbed on the biochar surface, serving as an interface to bind the nitrate anions and increase the amount of adsorption. This finding is consistent with the results of Zameni et al. (2016). The values of nitrate adsorption at six different concentrations for

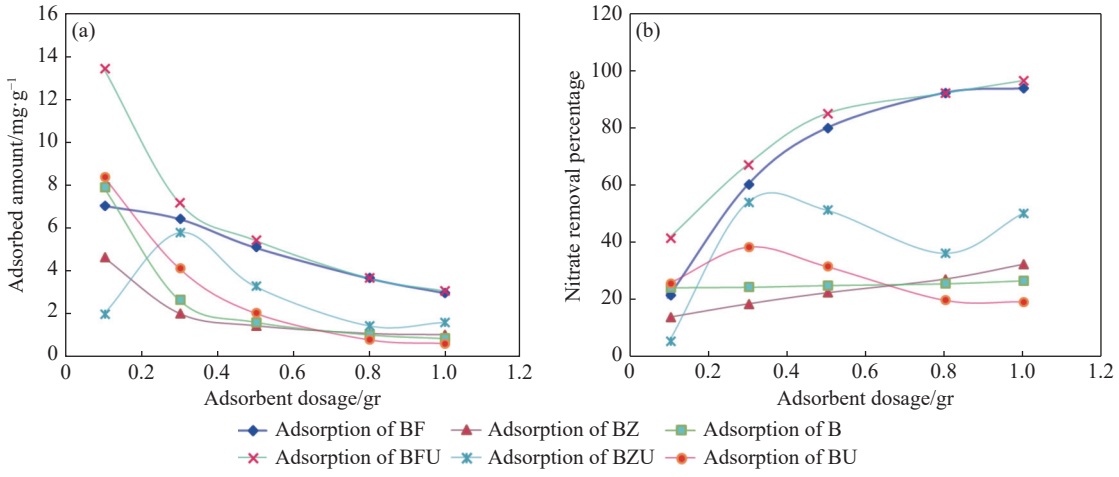

Fig. 3 The Amounts of nitrate adsorbed by B, BU, BZ, BZU, BF and BFU from solutions at different adsorbent doses

test treatments are presented in Table 1. Additionally, the efficiency and adsorption capacity at the equilibrium time, optimal pH, and adsorbent dose for different concentrations of nitrate solutions are illustrated in Fig. 4. As the concentration of dissolved nitrate increases, the loading ratio of ions on the adsorbent surface rises due to greater accessibility and more collisions of ions with the adsorbent surface, resulting in increased adsorption capacity (Amininejad et al. 2019). At low concentrations, nitrate ions effectively interact with the sites on the adsorbent surface, leading to a higher percentage of adsorption. However, at higher concentrations, the adsorption efficiency decreases due to the saturation of adsorption sites (Oprescu et al. 2022).

As the initial concentration increases, the adsorption capacity also increases, likely due to the concentration gradient and the higher driving force at higher concentrations. However, this leads to the saturation of all adsorption sites, resulting in a relative decrease in the total adsorbed nitrate efficiency. To determine the optimal concentration considering favorable efficiency and adsorption, a limit should be considered that removes the maximum amount of pollutant with the lowest cost (e.g., adsorbent usage, dilution of polluted sources, etc.). Based on this, the optimal concentration for

Table 1 Nitrate adsorption values in 6 different concentrations by experimental treatment

Initial concentration (mg/L)	BF		BFU		BZ		BZU		B		BU	
	C_e^{**} (mg/L)	q_e^{*} (mg/g)	C_e (mg/L)	q_e (mg/g)	C_e (mg/L)	q_e (mg/g)	C_e (mg/L)	q_e (mg/g)	C_e (mg/L)	q_e (mg/g)	C_e (mg/L)	q_e (mg/g)
20	0.03	0.79	0.19	0.79	4.48	0.62	13.81	0.82	12.48	0.30	13.24	0.90
45	1.16	1.75	1.36	1.74	21.14	0.95	35.28	1.29	36.43	0.34	24.28	2.76
80	6.40	2.94	5.27	2.98	53.87	1.04	54.21	3.43	60.74	0.77	39.98	5.33
100	8.57	3.65	14.73	3.41	74.00	1.03	64.18	4.77	77.20	0.91	49.67	6.71
150	23.78	5.04	36.81	4.52	112.06	1.51	64.71	11.37	107.75	1.68	87.49	8.33
200	46.14	6.15	49.96	6.00	151.51	1.93	129.02	9.46	122.79	3.08	105.88	12.54

Notes: q_e^{*} is the amount of nitrate adsorbed per unit weight of biochar
C_e^{**} is the equilibrium concentration of nitrate in solution

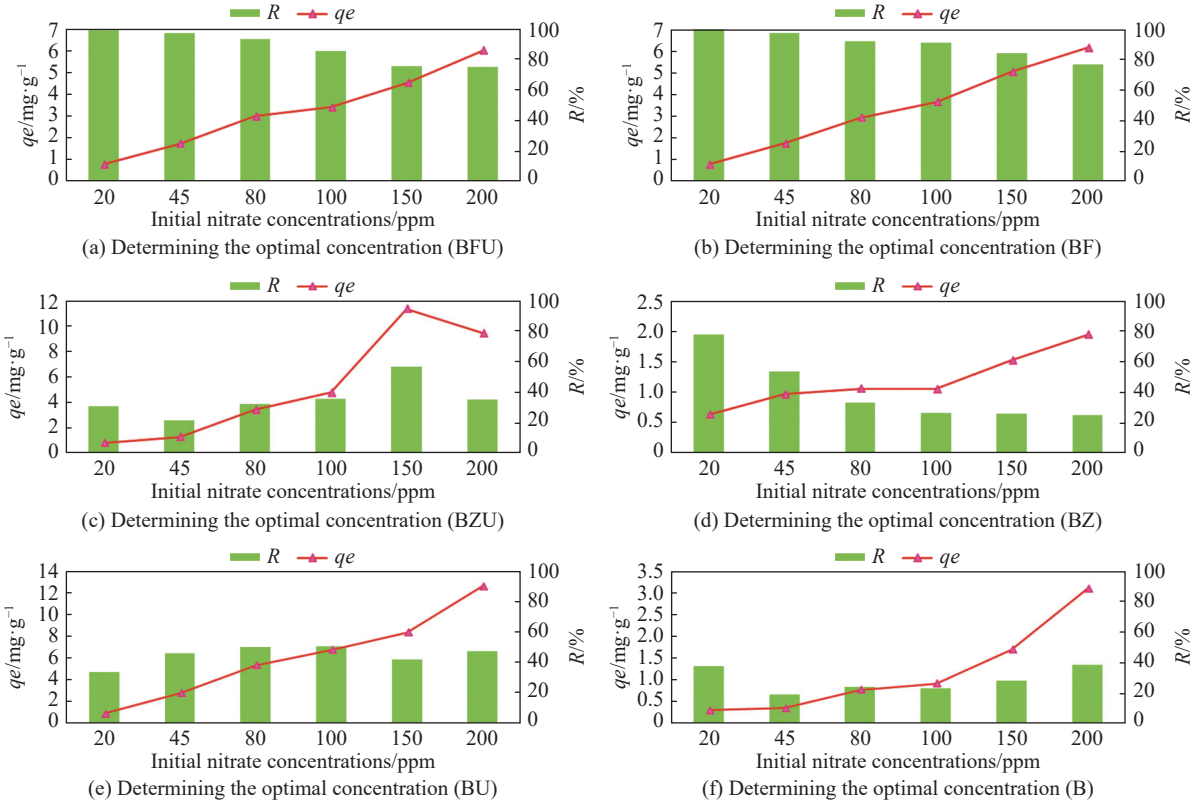

Fig. 4 The efficiency values and adsorption capacity at different nitrate concentrations

BFU was found to be 100 ppm, with corresponding efficiency and adsorption capacity values of 85.26% and 3.41 mg/g, respectively. Similarly, the optimal concentration for BF was determined to be 100 ppm, with efficiency and adsorption capacity values of 91.42% and 3.65 mg/g, respectively. For BZU, the optimal concentration is 150 ppm, resulting in efficiency and adsorption capacity values of 56.85% and 11.37 mg/g. For BZ, BU, and B, the optimal concentrations are 80 ppm, 200 ppm, and 200 ppm, with corresponding efficiency and adsorption capacity values of 32.66% and 1.04 mg/g, 47.05% and 12.54 mg/g, and 38.6% and 3.08 mg/g, respectively.

2.6 Investigation of nitrate adsorption isotherms

In recent years, the meticulous selection and application of adsorption isotherm models have become increasingly vital in accurately characterizing nitrate adsorption processes (González-López et al. 2021). Adsorption isotherms illustrate the interactions between the adsorbent and the adsorbed material, indicating that the amount of adsorption is a function of the adsorbate concentration. Among the isotherm models, Langmuir and Freundlich are the most commonly used in adsorption experiments. The Langmuir model is particularly relevant for monolayer adsorption, assuming adsorption occurs on an adsorbent surface with uniform energy and a limited number of adsorption sites. On the other hand, the Freundlich isotherm model is an empirical model suitable for non-uniform adsorption on independent sites, allowing for multiple layers of adsorption (Ogata et al. 2015).

The values obtained for Langmuir and Freundlich isotherm parameters, along with the correlation coefficient (R^2) of nitrate adsorption in different treatments, are presented in Table 2.

In the analysis of the two isotherms, it was observed that the Freundlich isotherm exhibited higher correlation coefficients (R^2) for BF, BFU, BZ, and B, indicating a better fit of the Freundlich model in these treatments. The better fit of the Freundlich adsorption isotherm suggests the heterogeneity of biochar surface adsorption sites, implying that the adsorption process is not limited to a single monolayer. Nitrate adsorption on the biochar surface is likely dominated by electrostatic adsorption and ion exchange. On the other hand, in the BZU and BU treatments, the Langmuir model showed a better fit according to the R^2 values. This indicates that in BU and BZU, the adsorption surfaces are likely uniform, and the adsorption process takes place in homogeneous regions on the adsorbent surfaces. Furthermore, the reaction between the adsorbing materials is limited, and after a single-layer adsorption on the adsorbent surface, the nitrate ions occupy all available sites, leading to no further adsorption on the adsorbent surface. In the examination of the Freundlich isotherm, the values of n_f (which are between 2 and 10) indicate the distribution of particles of adsorbed material on the surface of the adsorbent material. It was found that treatments BF, BFU, and BZU exhibit a favorable adsorption status, indicating the desirability of their curved shape. In treatment B, the value of n_f being between 1 and 2 indicates a normal adsorption state, and the curve shape is linear. Recent studies have shown that nitrate adsorption on various biochars and functionalized materials exhibits isotherm behaviors indicating high affinity between nitrate ions and adsorbent surfaces. For example, Eissa et al. (2024) found that adsorption data for different types of biochars fit both Langmuir and Freundlich isotherm models, with correlation coefficients (R^2) greater than 0.987, indicating strong interaction between nitrate ions and adsorbent surfaces. Similarly, Sharma and Gupta

Table 2 The values obtained for Langmuir and Freundlich isotherm parameters and the correlation coefficient of nitrate adsorbed in different treatments

Isotherms parameters						
Treatment	Langmuir			Freundlich		
	q_m	b	R^2	k_f	n_f	R^2
BF	3.345	8.491	0.894	1909.414	3.641	0.985
BFU	3.664	1.405	0.95	1484.22	2.942	0.981
BZ	1.341	0.184	0.806	386.63	3.562	0.856
BZU	-	-	0.886	26.24	0.795	0.799
B	1.632	0.016	0.713	18.488	1.047	0.806
BU	-	-	0.946	56.48	0.852	0.944

(2024) reported that the Sips isotherm model provided the best fit for nitrate adsorption on iron-coated biochar derived from parthenium Hysterophorus, indicating heterogeneous adsorption sites with high affinity for nitrate ions. For BU and BZU, n_f values less than 1 suggest a weak adsorption state and an unfavorable curve shape. The high values of adsorption capacity (k_f) obtained for BF, BFU, and BZ, which are 1,909.414, 1,484.22, and 386.63, respectively, indicate the high adsorption capacity of these adsorbents for nitrate. Fig. 4 displays the curves of adsorption isotherms. Recent studies have demonstrated that the shape of adsorption isotherms provides insights into the affinity between adsorbents and nitrate ions. For instance, Homagai et al. (2023) investigated the adsorption of nitrate and nitrite anions using modified maize stalks and observed that the adsorption data conformed well to the Langmuir isotherm model, indicating monolayer adsorption with high affinity at low concentrations. In contrast, according to Fig. 5, the adsorption isotherm curve for BZU is S-shaped. S-type isotherms show that with the increase in the concentration of the adsorbed substance (pollutant), the slope initially increases, but eventually, as the empty adsorption sites are filled, the slope decreases and reaches zero.

2.7 Investigating the effect of ultrasonic waves on nitrate adsorption

The highest values for maximum adsorption capacity (q_m) were obtained in BFU and BF, which are 3.664 mg/g and 3.345 mg/g, respectively, indicating that ultrasonication increased the amount of q_m. Interestingly, the equilibrium time for BFU (5 min) was much shorter than that of BF (60 min). Moreover, when comparing the values of R^2 in the Langmuir and Freundlich models, it was observed that the use of ultrasonics increases the values of R^2 in the Langmuir model and decreases them in the Freundlich model. This observation suggests that ultrasonication leads to uniformity in the adsorption surfaces, causing the adsorption process to occur in homogeneous regions on the adsorbent surfaces and resulting in single-layer adsorption on the adsorbent surface.

This effect might be attributed to the pulverization of the adsorbent particles in the nitrate solution due to the application of ultrasonic waves. The experiments revealed that the adsorbent particles turned into a very soft, tiny, and homogeneous powder during the BFU, BZU, and BU tests, an effect not observed when the solutions were merely shaken in B, BZ, and BF. The percentage of nitrate removed in different treatments and experiments is shown in Table 3. Comparing the percentage of nitrate removal in the experiments to determine the optimal pH, it was observed that ultrasonic waves had a significant effect on nitrate removal and increased the removal percentage for BU compared to B and for BZU compared to BZ. Similar results were found in the experiments to determine the optimal adsorbent dose, where ultrasonication increased the percentage of nitrate removal in all three adsorbents.

Furthermore, in the experiments with different initial nitrate concentrations, ultrasonication also led to an increase in the percentage of nitrate

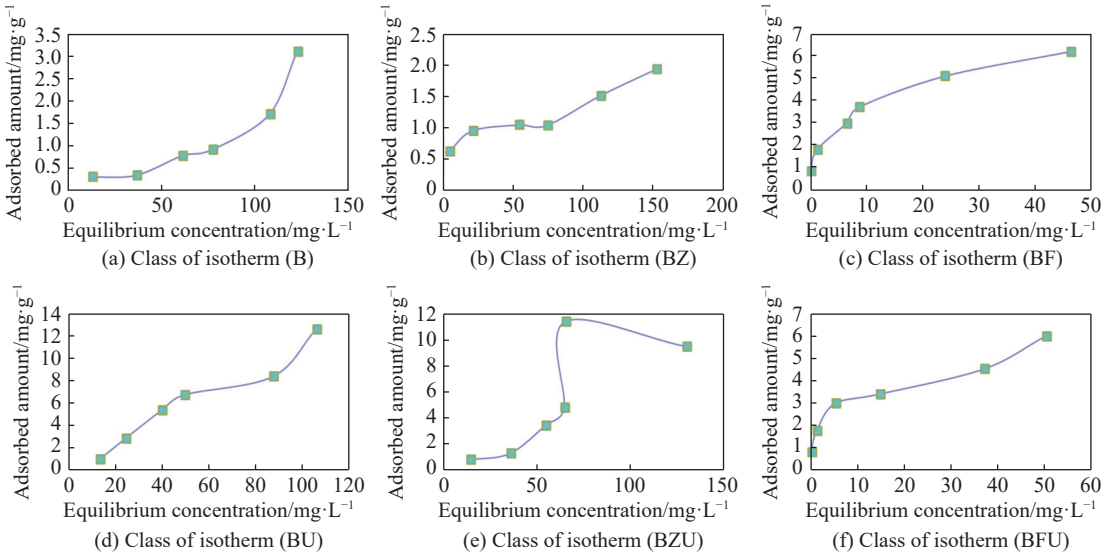

Fig. 5 The amount of nitrate adsorbed by B, BU, BZ, BZU, BF, and BFU from solutions at different initial nitrate concentrations

Table 3 Percentage of nitrate removal in different treatments and experiments

Nitrate removal percentage						
pH	BF	BFU	BZ	BZU	B	BU
2	74.39	71.70	30.19	13.99	14.75	38.91
4	84.37	76.94	22.55	24.06	4.82	33.58
6	76.49	74.30	15.03	20.29	1.50	16.67
7	82.97	77.96	11.46	18.01	1.40	9.79
8	80.11	73.59	5.91	20.23	0.96	9.15
10	65.49	72.42	16.18	27.34	7.61	26.43
Adsorbent Dosage (gr)						
0.1	22.11	42.12	14.58	6.239	24.79	26.31
0.3	60.57	67.65	19.20	54.46	24.96	38.87
0.5	80.19	85.26	23.04	51.77	25.53	32.19
0.8	92.42	92.34	27.77	36.76	26.16	20.48
1	94.02	96.72	32.90	50.59	27.18	19.91
Initial nitrate concentrations						
20	99.81	99.04	77.55	30.90	37.58	33.76
45	97.40	96.95	53.01	21.59	19.02	46.03
80	91.99	93.41	32.66	32.23	24.06	50.01
100	91.42	85.26	25.99	35.81	22.79	50.32
150	84.14	75.45	25.29	56.85	28.16	41.67
200	76.92	75.01	24.24	35.48	38.60	47.05

removal in BU and BZU. Analyzing the data in Table 1, we found that ultrasonication resulted in an increase in the adsorption capacity values in biochar and biochar adsorbents coated with Zn^{2+} and a decrease in the final concentration of nitrate in the solution.

In treatment U, the results showed that ultrasound can remove nitrate from aqueous solutions, which can be attributed to the production of hydrogen from ultrasound products in aqueous solutions (at high frequencies of 20 kHz), which causes the reduction of nitrate ions and free radicals produced in the microstreaming process as well as the high temperature and pressure of microbubbles and the high energy of ultrasonic irradiation that promotes bond cleavage. In the ultrasonic process, pyrolysis occurs within the cavities of water molecules, which produces hydroxyl radicals and hydrogen atoms in the gas phase. When contaminants come into contact with ultrasonic waves, the contaminants react with hydroxyl radicals or decompose due to heat (Alashti et al. 2024).

3 Conclusion

The performance of BF and BFU treatments was excellent, with the removal efficiency of nitrate from aqueous solutions reaching over 90% in many experiments. The use of ultrasonic waves for 5 minutes showed promising results compared to tests without ultrasonics. It led to increased nitrate removal, higher adsorption capacity, and enhanced maximum adsorption capacity. Additionally, ultrasonication contributed to creating uniformity of the adsorption surfaces, among other beneficial effects. Utilizing ultrasonic waves in this clean and environmentally friendly process can play a crucial role in addressing pollutants like nitrate and mitigating their harmful impacts. Further research on the effects of these waves on environmental phenomena is warranted to fully explore their potential. Furthermore, the integration of ultrasonic waves with iron-coated biochar was evaluated for its cost-effectiveness. Despite the added energy requirement for ultrasonication, the significant improvement in nitrate removal efficiency and reduction in equilibrium time make this combined method economically viable, especially considering the low-cost raw material (rice straw) used for biochar production.

List of nonstandard abbreviations

B: Treatments using biochar adsorbent

BU: Application of biochar adsorbent combined with ultrasonic waves

BZ: Biochar coated with Zn^{2+}

BZU: Biochar coated with Zn^{2+} combined with ultrasonic treatment

BF: Biochar coated with Fe^{3+}

BFU: Biochar coated with Fe^{3+} combined with ultrasonic treatment

U: Ultrasonic without adsorbent

References

Alashti MR, Khoshravesh M, Sadegh-zadeh F, et al. 2024. The effect of ultrasonic waves on nitrate removal in aqueous solution. Iranian Journal of Irrigation and Drainage, 2(18): 319−328.

Amininejad M, Boroomand-Nasab S, Moazed H, et al. 2019. Evaluation of nitrate removal from aqueous solution by nanostructure of Conocarpus. Scientific Research Journal of Irrigation and Water Engineering of Iran, 37: 167−180. DOI：10.22125/iwe.2019.95882.

APHA. 2012. Standard Methods for the Examination of Water and Wastewater. 22nd Edition, American Public Health Association, Washington DC.

Cataldo DA, Maroon M, Schrader LE, et al. 1975. Rapid colorimetric determination of nitrate in plant tissues by nitration of salicylic acid. Communication of Soil Science and Plant Analysis, 6(1): 71−80. DOI：10.1080/00103627509366547.

Dehghani MH, Karri RR, Koduru JR, et al. 2023. Ultrasonic cavitation: Tackling organic pollutants in wastewater. Ultrasonics Sonochemistry, 94: 106302.

Eissa R, Jeyakumar L, McKenzie DB, et al. 2024. Influence of biochar feedstocks on nitrate adsorption capacity. Earth, 5(4): 1080−1096. DOI：10.3390/earth5040055.

González-López J, Hu X, Rajahmundry R, et al. 2021. Critical evaluation of isotherm modeling in nitrate adsorption studies. Water, Air, and Soil Pollution, 232(7): 1−15. DOI：10.1007/s11270-021-05345-6.

Guo F, Zhang Y, Li H. 2023. The removal of ammonia-nitrogen from aquaculture water based on cavitation effect of ultrasonic vibration. Journal of Vibroengineering, 25(5): 1012−1020. DOI：10.21595/vp.2023.23575extrica.com.

Homagai PL, Poudel R, Paudyal H, et al. 2023. Adsorption of nitrate and nitrite anion by modified maize stalks from aqueous solutions. Environmental Science and Pollution Research, 30: 54682−54693. DOI：10.1007/s11356-023-26179-y.

Hosseingholilu B, Banakar A, Mostafaei M. 2019. Design and evaluation of a novel ultrasonic desalination system by response surface methodology. Desalination and Water Treatment, 164: 263−275. DOI：10.5004/dwt.2019.24458.

Hu Q, Chen N, Feng C, et al. 2015. Nitrate adsorption from aqueous solution using granular chitosan-Fe^{3+} complex. Journal of Applied Surface Science, 374: 1−9. DOI：10.1016/j.apsusc.2015.04.049.

Janajreh I, Ali U, Hawwa M. 2022. Sonicated direct contact membrane distillation: Influence of sonication parameters. Desalination, 533: 115779. DOI：10.1016/j.desal.2022.115779.

Kumar R, Singh R. 2024. Removal of nitrate ion from aqueous solution using palmyrah nut shell activated carbon: Factorial optimization and equilibrium studies. Discover Civil Engineering, 2(1): 54. DOI：10.1007/s44290-024-00054-2.

Lahjouj A, Hmaidi AE, Bouhafa K. 2020. Spatial and statistical assessment of nitrate contamination in groundwater: Case of Sais Basin, Morocco. Journal of Groundwater Science and Engineering, 8(2): 143−157. DOI：10.19637/j.cnki.2305-7068.2020.02.006.

Mohamad Aris KH, Ramli S, Othman Z, et al. 2018. Evaluation of ammonia-nitrogen removal by ultrasonic irradiation in synthetic solution using response surface methodology. Key Engineering Materials, 797: 108−117. DOI：10.4028/www.scientific.net/KEM.797.108.

Mood SH, Pelaez-Samaniego MR, Han Y, et al. 2024. Iron- and nitrogen-modified biochar for nitrate adsorption from aqueous solution. Sustainability, 16(13): 5733. DOI：10.3390/su16135733.

Nguyen Le KT, Maldonado JFG, Nguyen TL, et al. 2024. The short-term effect of nitrogen on freshwater cyanobacteria and cyanotoxins. Frontiers in Water, 6: 1432183. DOI：10.3389/frwa.2024.1432183.

Ogata F, Imai D, Kawasaki N. 2015. Adsorption of nitrate and nitrite ions onto carbonaceous material produced from soybean in a binary solution system. Journal of Environmental Chemical Engineering, 3: 155−161. DOI：10.1016/j.jece.2014.11.025.

Oprescu EE, Enascuta EC, Vasilievici G, et al. 2022. Preparation of magnetic biochar for nitrate removal from aqueous solutions. Reaction Kinetics, Mechanisms and Catalysis, 135(3): 1647−1665. DOI：10.1007/s11144-022-02263-1.

Rashwan SS, Dincer I, Mohany A. 2020. An investigation of ultrasonic based hydrogen production. International Journal of Hydrogen Energy, 205: 118006. DOI：10.1016/j.energy.2020.118006.

Reusch TBH, Dierking J, Andersson HC, et al. 2018. The Baltic Sea as a time machine for the future coastal ocean. Science Advances, 4: 8195. DOI：10.1126/sciadv.aar8195.

Serna-Galvis EA, Porras J, Torres-Palma RA. 2022. A critical review on the sonochemical degradation of organic pollutants in urine,

seawater, and mineral water. Ultrasonics Sonochemistry, 82: 105861. DOI：10.1016/j.ultsonch.2021.105861.

Sharma A, Gupta S. 2024. Parthenium hysterophorus-derived iron-coated biochar: A sustainable solution for nitrate and phosphate removal from water. Biomass Conversion and Biorefinery, 14(3): 821. DOI：10.1007/s13399-024-05821-w.

Ward MH, Jones RR, Brender JD, et al. 2024. Drinking-water nitrate and human health: An updated review. Environmental Science & Technology, 58(4): 2345−2357.

Zameni L, Sadegh-zadeh F, Seh-Bardan BJ. 2016. Nitrate leaching in soil modified by biochar and iron coated biochar. M.S. thesis, Sari Agricultural Sciences and Natural Resources University.

Zhang M, Song G, Gelardi DL, et al. 2020. Evaluating biochar and its modifications for the removal of ammonium, nitrate, and phosphate in water. Water Research, 186: 116303. DOI：10.1016/j.watres.2020.116303.